

General Disclaimer

One or more of the Following Statements may affect this Document

- This document has been reproduced from the best copy furnished by the organizational source. It is being released in the interest of making available as much information as possible.
- This document may contain data, which exceeds the sheet parameters. It was furnished in this condition by the organizational source and is the best copy available.
- This document may contain tone-on-tone or color graphs, charts and/or pictures, which have been reproduced in black and white.
- This document is paginated as submitted by the original source.
- Portions of this document are not fully legible due to the historical nature of some of the material. However, it is the best reproduction available from the original submission.

161
Mr. Harry Buchanan

MAGNETIC FLUID SIMULATION OF LIQUID SLOSHING IN LOW GRAVITY

by

Franklin T. Dodge

Luis R. Garza

TECHNICAL REPORT NO. 9

Contract No. NAS8-20290

Control No. DCN 1-9-75-10050(1F)

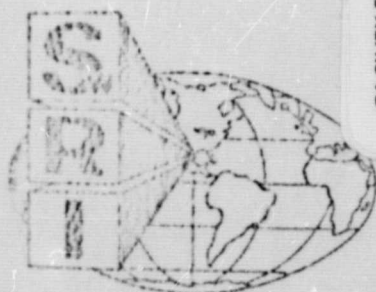
SwRI Project 02-1846

Prepared for

George C. Marshall Space Flight Center
National Aeronautics and Space Administration
Marshall Space Flight Center, Alabama

August 1970

FACILITY FORM 602	<u>N70-42167</u>	
	(ACCESSION NUMBER)	(THRU)
	<u>36</u>	<u>1</u>
	(PAGES)	(CODE)
	<u>CR-102869</u>	<u>12</u>
	(NASA CR OR TMX OR AD NUMBER)	(CATEGORY)



SOUTHWEST RESEARCH INSTITUTE
SAN ANTONIO HOUSTON

Reproduced by
NATIONAL TECHNICAL
INFORMATION SERVICE
Springfield, Va. 22151

SOUTHWEST RESEARCH INSTITUTE
Post Office Drawer 28510, 8500 Culebra Road
San Antonio, Texas 78228

MAGNETIC FLUID SIMULATION OF LIQUID SLOSHING IN LOW GRAVITY

by

Franklin T. Dodge
Luis R. Garza

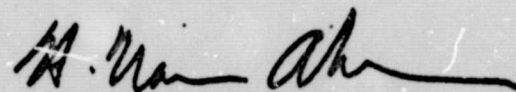
TECHNICAL REPORT NO. 9
Contract No. NAS8-20290
Control No. DCN 1-9-75-10050(1F)
SwRI Project 02-1846

Prepared for

George C. Marshall Space Flight Center
National Aeronautics and Space Administration
Marshall Space Flight Center, Alabama

August 1970

Approved:



H. Norman Abramson, Director
Department of Mechanical Sciences

ACKNOWLEDGEMENTS

The authors thank the following personnel of NASA-LeRC:
Mr. James E. Lawrence for making the NASA-electromagnet facility available to us; Mr. Charles Lizanich and Mr. Erwin Meyn for running the electromagnet and helping us to set up the tests; and Mr. Stephen Papell and Mr. Otto Faber for letting us use generous amounts of their magnetic-colloid liquid. We also thank Dr. George Matzkanin of SwRI for his help in computing saturation magnetic fields of a magnetic-colloid liquid.

SUMMARY

An exploratory series of tests of simulated low-gravity liquid sloshing using a magnetic-colloid liquid in conjunction with a solenoidal magnetic field is described herein. A description of the experimental apparatus and test procedure is also presented.

The magnetic body-force exerted on the liquid was varied by changing the magnetic field strength in order to obtain effective gravity levels as small as 0.01 g. The measured slosh natural frequencies for both cylindrical and spherical tanks in these low-gravity conditions agreed very well with theoretical predictions. Slosh damping, however, was significantly larger than expected because of the increase in viscosity of magnetic liquids due to magnetic field effects.

A magnetic-fluid analysis of sloshing is presented, and indicates that some deviation from true low-gravity behavior might occur whenever the Bond number is smaller than one. The discrepancy is caused by a magnetic interaction at the free surface that induces a jump in liquid pressure similar to that induced by surface tension.

TABLE OF CONTENTS

	<u>Page</u>
LIST OF ILLUSTRATIONS	v
LIST OF SYMBOLS	vi
I. INTRODUCTION	1
II. EXPERIMENTAL SETUP, TEST PROCEDURES, AND DATA REDUCTION	2
A. Experimental Setup	2
B. Test Procedure	5
C. Data Reduction	10
III. TEST RESULTS	12
A. Natural Frequency	12
B. Slosh Damping	12
IV. THEORY	18
A. Basic Equations	18
B. Magnetic Body-Force Potential	18
C. Equilibrium Free Surface	21
D. Sloshing Analysis	23
V. CONCLUSIONS AND RECOMMENDATIONS	24
LIST OF REFERENCES	25

LIST OF ILLUSTRATIONS

<u>Figure</u>		<u>Page</u>
1	Sectional View of NASA-LeRC Electromagnet	3
2	Schematic of Experimental Apparatus	4
3	Capacitive Probe for Cylindrical Tank	6
4	Spherical Tank and Cylindrical Guide Tube	7
5	View of Test Setup	8
6	Test Instrumentation	9
7	Natural Frequency, 2.00-in. Cylindrical Tank	13
8	Natural Frequency, 1.50-in. Cylindrical Tank	14
9	Natural Frequency, 1.00-in. Cylindrical Tank	15
10	Natural Frequency, 2.125-in. Spherical Tank, Half-Full	16
11	Natural Frequency, 2.125-in. Spherical Tank, Three-Quarters Full	17
12	Slosh Damping, 1.50-in. Cylindrical Tank	19
13	Slosh Damping, 2.125-in. Spherical Tank, Three-Quarters Full	20
14	Nomenclature for Analysis	22

LIST OF SYMBOLS

Symbol	Definition
$\vec{a}_z, \vec{a}_r, \vec{n}$	unit vectors in r, z, and free-surface normal directions
\vec{B}	applied magnetic induction field (webers/meter ²)
B_0	axial magnetic field at center of magnet
B_r, B_z	radial and axial components of \vec{B}
$f(r)$	equilibrium free surface height
$F(R)$	dimensionless free surface height, f/R_0
g	standard gravitational acceleration
g_{eff}	effective gravity acting on liquid
g_{mag}	apparent decrease in g created by magnetic body-force
h	average depth of liquid in cylindrical tank
$H(R, \theta)$	dimensionless wave height, $\eta\Omega/R_0 \sin \omega t$
\vec{M}	magnetization of magnetic liquid (amperes/meter)
M_n	component of \vec{M} normal to free surface, $\vec{M} \cdot \vec{n}$
M_0	magnitude of \vec{M}
N_{BO}	Bond number, $\rho g_{\text{eff}} R_0^2 / \sigma$
N_{GA}	Galileo number, $R_0^{3/2} g_{\text{eff}}^{1/2} / \nu^{1/2}$
N_{MI}	magnetic interaction number, $\mu_0 M_0^2 R_0 / 2\sigma$
p	liquid pressure
r, z, θ	cylindrical coordinate axes
R, Z	dimensionless coordinate axes, $r/R_0, z/R_0$
R_0	tank radius

LIST OF SYMBOLS (Cont'd)

Symbol	Definition
R_1, R_2	principal radii of curvature of free surface
t	time
\vec{V}	velocity vector of liquid
δ	logarithmic decrement of slosh amplitude
$\eta(r, \theta, t)$	slosh wave height
μ_0	permeability of free space, $4\pi \times 10^{-7}$ (webers/ampere-meter)
ν, ρ, σ	kinematic viscosity, density, and surface tension
τ	dimensionless time, $t(\sigma/\rho R_0^3)^{1/2}$
$\phi(r, \theta, z, t)$	velocity potential
$\Phi(R, \theta, Z)$	dimensionless velocity potential, $\phi(\rho/\sigma R_0)^{1/2}/\cos \omega t$
$\psi(r, z)$	magnetic body-force potential
ω	slosh natural frequency
Ω	dimensionless natural frequency, $\omega(\rho R_0^3/\sigma)^{1/2}$

I. INTRODUCTION

An experimental study of liquid free-surface motions in a low-gravity environment continues to be a difficult problem for the simple reason that there is no suitable "laboratory." Several low-gravity simulation techniques have been developed, but, although useful in certain special cases, they all possess major limitations such as short test duration or magnification of viscous effects. One apparent exception is the "magnetic fluid" technique used by Papell and Faber to study reduced-gravity boiling, Ref. 1, and proposed by Dodge some time ago as a technique of general usefulness, Ref. 2. In this method, an ordinary solvent such as n-heptane is made magnetizable by dispersing in it submicron particles of magnetic iron oxide to form an extremely stable, low-viscosity colloidal system. The liquid can then be partially or completely levitated in a magnetic field. This seems to have been demonstrated first by Rosenweig and co-workers, who coined the name "ferrohydrodynamics" for this general field, Refs. 3, 4, and 5.

The optimistic evaluation of the magnetic fluid simulation presented by Dodge, Ref. 2, was based primarily on the discussion given by Papell and Faber in Refs. 1 and 6. They showed in essence that the body force exerted on the magnetic fluid by the magnetic field is $\vec{M} \cdot \nabla \vec{B}$ where \vec{M} is the magnetization of the fluid, and $\nabla \vec{B}$ is the gradient of the applied magnetic induction field, \vec{B} . According to Papell and Faber, the quantity $\vec{M} \cdot \nabla \vec{B}$ can be (1) made nearly constant throughout the fluid and (2) directed in opposition to the normal gravity vector, by using a large, well-designed solenoidal magnet. In other words, it seemed possible to achieve a true low-gravity simulation for an extended period of time by the magnetic fluid method.

To determine if this is true and to evaluate the usefulness of the method, we conducted a series of exploratory experiments in simulated low-gravity liquid sloshing. The primary objectives of these tests were to measure the slosh natural frequency and smooth-wall viscous damping as a function of the simulated gravity level in tank configurations for which theories and experimental confirmations were already available to compare with our results; a secondary objective was to determine the nonlinear effect of slosh amplitude on natural frequency.

We have also developed a magnetic-fluid-dynamics theory of sloshing in a solenoidal magnetic field, based on the general theory given by Curtis, Ref. 7. Our theory demonstrates that several magnetically-induced forces, in addition to the gravity-cancelling force, limit the accuracy of the simulation; these forces cannot be totally eliminated, regardless of the type of magnetic field employed.

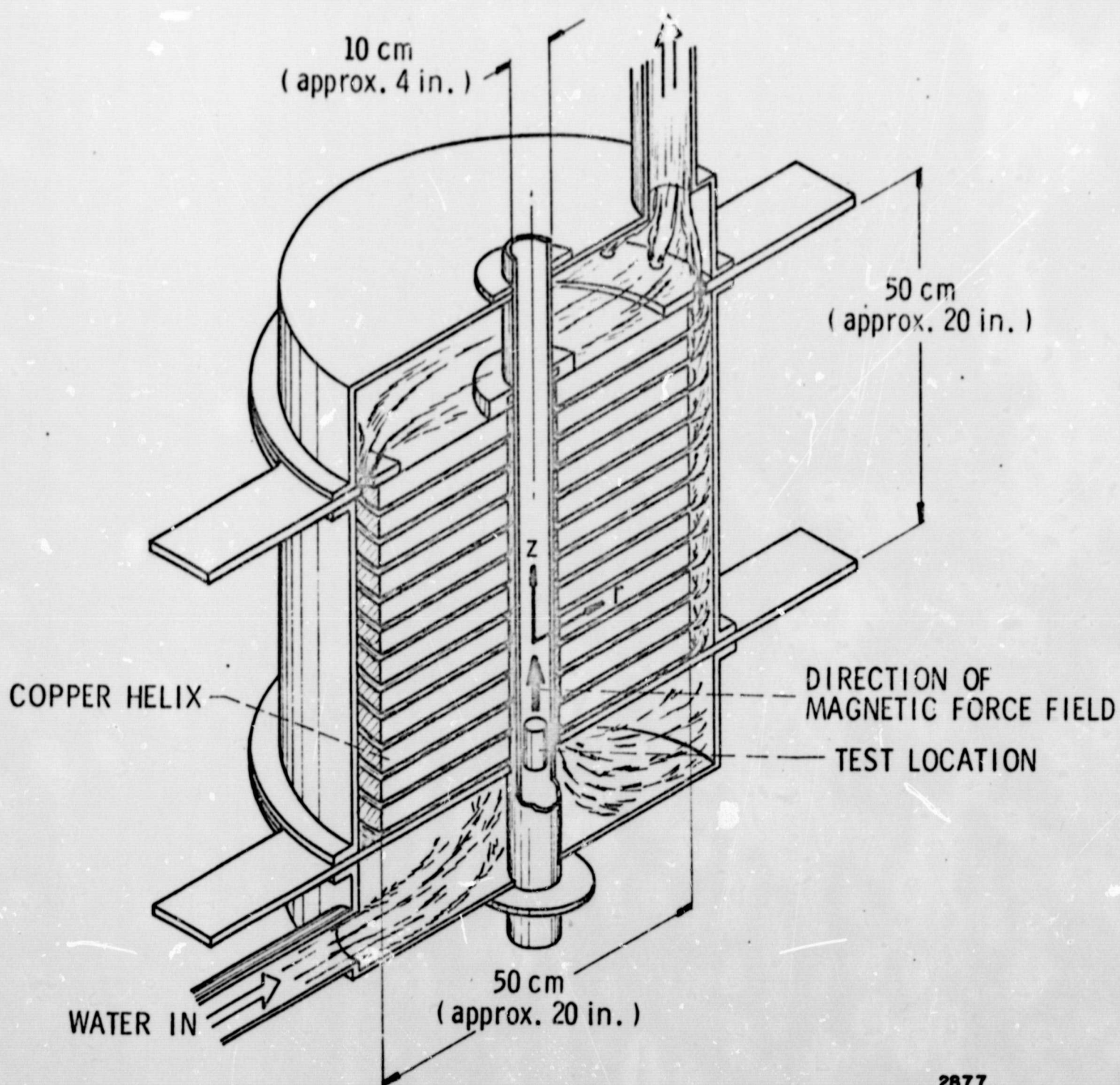
II. EXPERIMENTAL SETUP, TEST PROCEDURE, AND DATA REDUCTION

A. Experimental Setup

The 110-kilogauss (maximum) water-cooled, solenoidal electromagnet at NASA-Lewis Research Center was used to generate the required magnetic fields for the tests; this magnet is described schematically in Figure 1. Near the bottom of the magnet there is about 4 in. (10 cm) of axial length for which $\partial \vec{B} / \partial Z$ is constant over the entire bore; consequently, the test tanks were located at this point as recommended in Ref. 6.

Our experimental apparatus was designed to suspend a tank at the proper spot in the magnet, excite steady-state lateral sloshing of the liquid in the tank, record the slosh wave amplitude and its timewise decay after quick-stopping the tank, and determine the actual weight (including magnetic effects) of the liquid while the tests were in progress. The final configuration of this apparatus, after several modifications were made as the result of "trial runs" at NASA-LeRC prior to the final tests, is shown in Figure 2. In operation, the test tank was attached to an aluminum tube, approximately 31 in. long whose upper end was held firmly by a tight-fitting sleeve and set-screws bearing on grooves machined in the tube surface. This arrangement allowed the vertical position of the tank to be easily adjusted merely by sliding the tube up and down in the sleeve. Four beams, two each on opposite sides of the tube, supported the sleeve over the magnet bore. The beams were cantilevered from supports rigidly connected to a heavy plate which, in turn, was rigidly attached, by four columns, to the main shake table (the uppermost horizontal plate in Figure 2). Four cantilever-beam translation springs supported the shake table, which was driven horizontally by a "25-lb" electrodynamic shaker. The heavy base plate, to which the translation springs were attached, and the shaker were both bolted directly to a frame rigidly connected to the magnet frame. The entire structure was constructed of either aluminum or nonmagnetic stainless steel to minimize magnetic interferences. The beams supporting the sleeve/tube also served as a total deadweight gage of the tube, tank, and liquid. Semiconductor strain gages (gage factor ≈ 50), bonded to a milled 0.030-in.-thick section in the upper pair of beams, acted as the sensing elements to measure the beam deflections under the load of the tube-tank-liquid system.

Three cylindrical tanks, fabricated from acrylic plastic tubing, and one spherical tank, machined in two halves from Lucite[®], were used during the tests. The cylindrical tanks had diameters of 1.00, 1.50, and 2.00 in., and were filled to depths greater than one diameter, while the spherical tank, which had a diameter of 2.125 in., was tested one-half and three-quarters full.



2877

FIGURE 1. SECTIONAL VIEW OF NASA-LERC ELECTROMAGNET

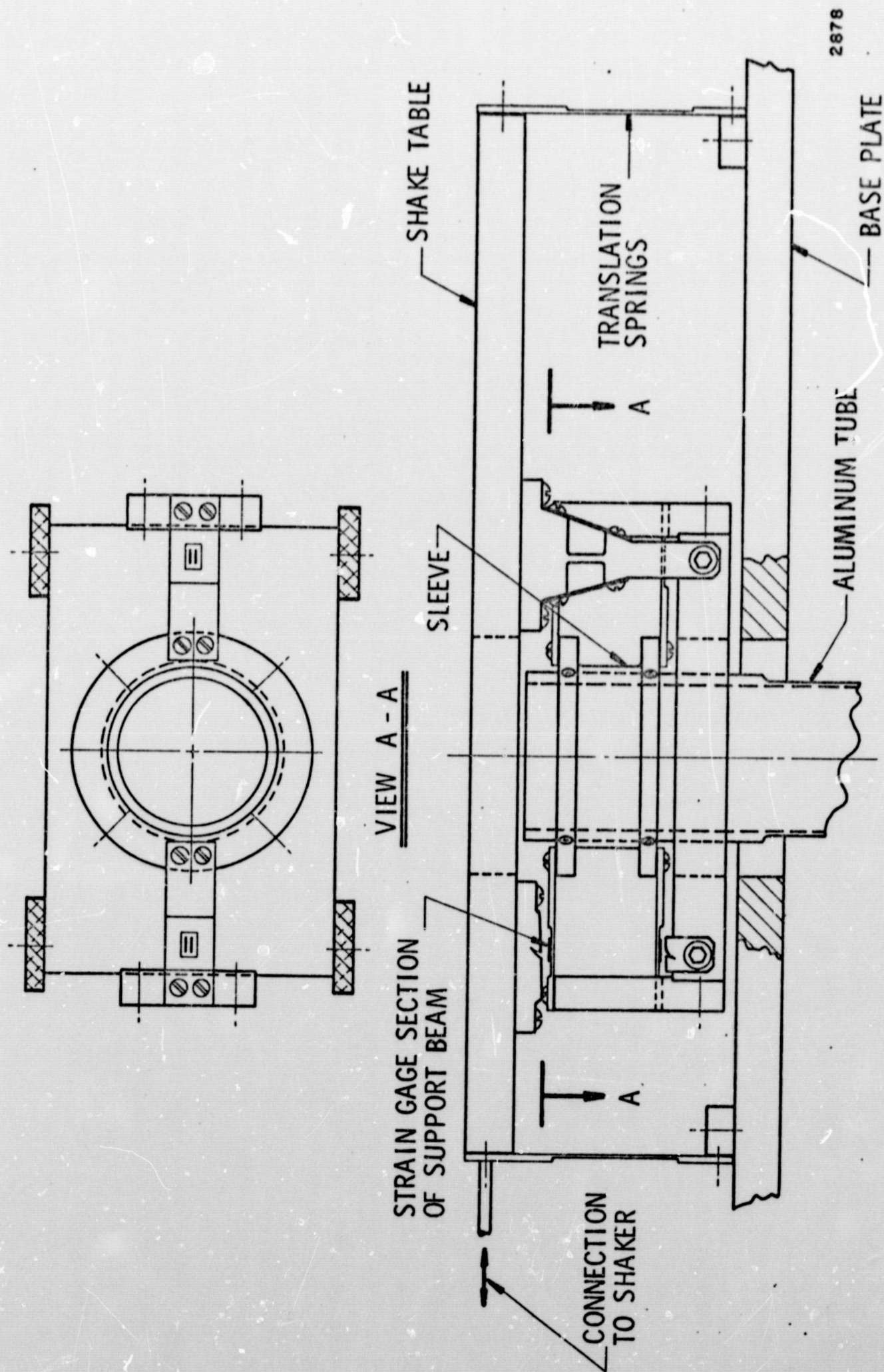


FIGURE 2. SCHEMATIC OF EXPERIMENTAL APPARATUS

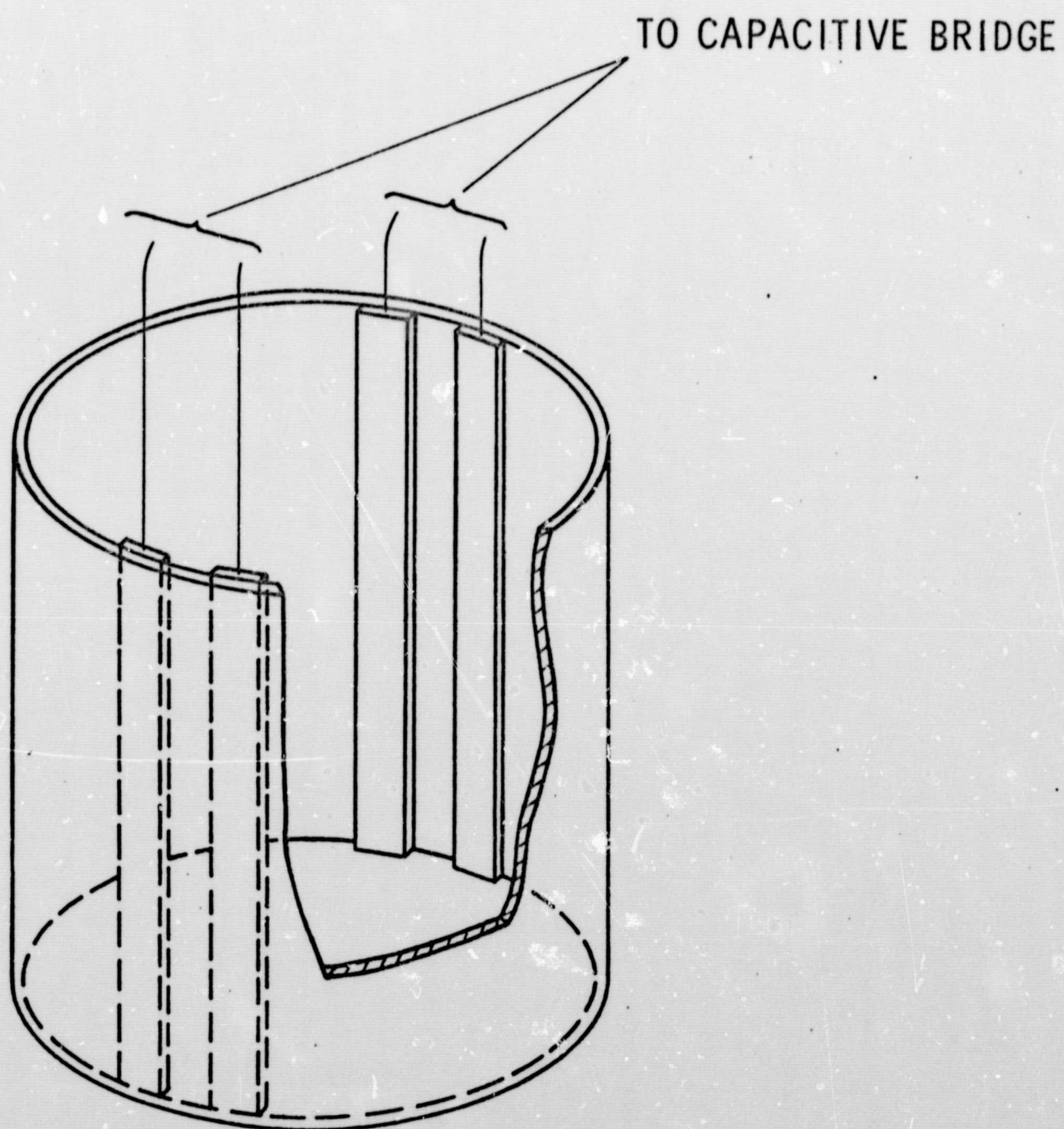
Capacitive probes in the tanks measured the slosh wave height. For the cylindrical tanks, two sets of two copper strips were attached along the tank walls as shown in Figure 3. (The thickness of the strips is exaggerated in Figure 3, for clarity.) The capacitance of each set of strips, measured by a capacitance bridge, varied with the total length of the strips immersed in the liquid. Since the strips were located at opposite ends of the particular tank diameter oriented in the direction of the excitation, one set of strips attained its maximum capacitance during the sloshing at the same instant as the other attained its minimum; this doubled the sensitivity that could be achieved by one set of strips. The spherical tank probes were silver-epoxy strips since it was difficult to make metallic copper strips conform to the spherical walls. We did not intend that the probes be used to measure slosh heights in an absolute sense because it was sufficient to have only an indication of wave motion that could be displayed on an oscilloscope.

B. Test Procedure

After filling the selected tank with a preweighed volume of liquid, the tank was attached to the long aluminum tube, as shown in Figure 4, and the tube inserted to the correct depth in the magnet bore, as shown in Figure 5; some care was taken to align the axis of the tube with the axis of the magnet bore. Electrical connections to the recording instrumentation, shown in Figure 6, were then made.

The deadweight gage was calibrated by adding small weights to the aluminum tube in order to deflect the supporting beams. The strain-gage readout on a digital voltmeter had a typical sensitivity of about 3-mV change in reading per gram of weight added; the "least count" of the voltmeter was 1 mV, so 0.3 gram was about the smallest weight change that could be discriminated. The calibration curve was always reasonably linear, but a DC drift in the readout appeared at irregular intervals, the cause of which was never completely discovered or eliminated. Further, the electrical gain, or amplification of the electronics needed to measure the small weight changes that we expected around a simulated zero-gravity, was so large that electrical "noise" caused the voltmeter reading to fluctuate by as much as 1 or 2 mV; thus, we always read the voltmeter at least four times in a space of a few seconds and took the average to be the true reading.

After attaching a dial indicator to the shake table to measure table displacements, we sloshed the liquid in the tank by exciting the shake table in sinusoidal motion. The resonant frequency was determined approximately by noting the excitation frequency that gave the largest slosh probe signal (amplitude) on the oscilloscope. We then determined resonance exactly by using the slosh probe signal and the shake-table amplitude signal together to form a Lissajous curve on the oscilloscope. Next, the tank was "quick-stopped" by disconnecting the DC field coils of the electrodynamic shaker



2879

FIGURE 3. CAPACITIVE PROBE FOR CYLINDRICAL TANK



FIGURE 4. SPHERICAL TANK AND CYLINDRICAL GUIDE TUBE



FIGURE 5. VIEW OF TEST SETUP

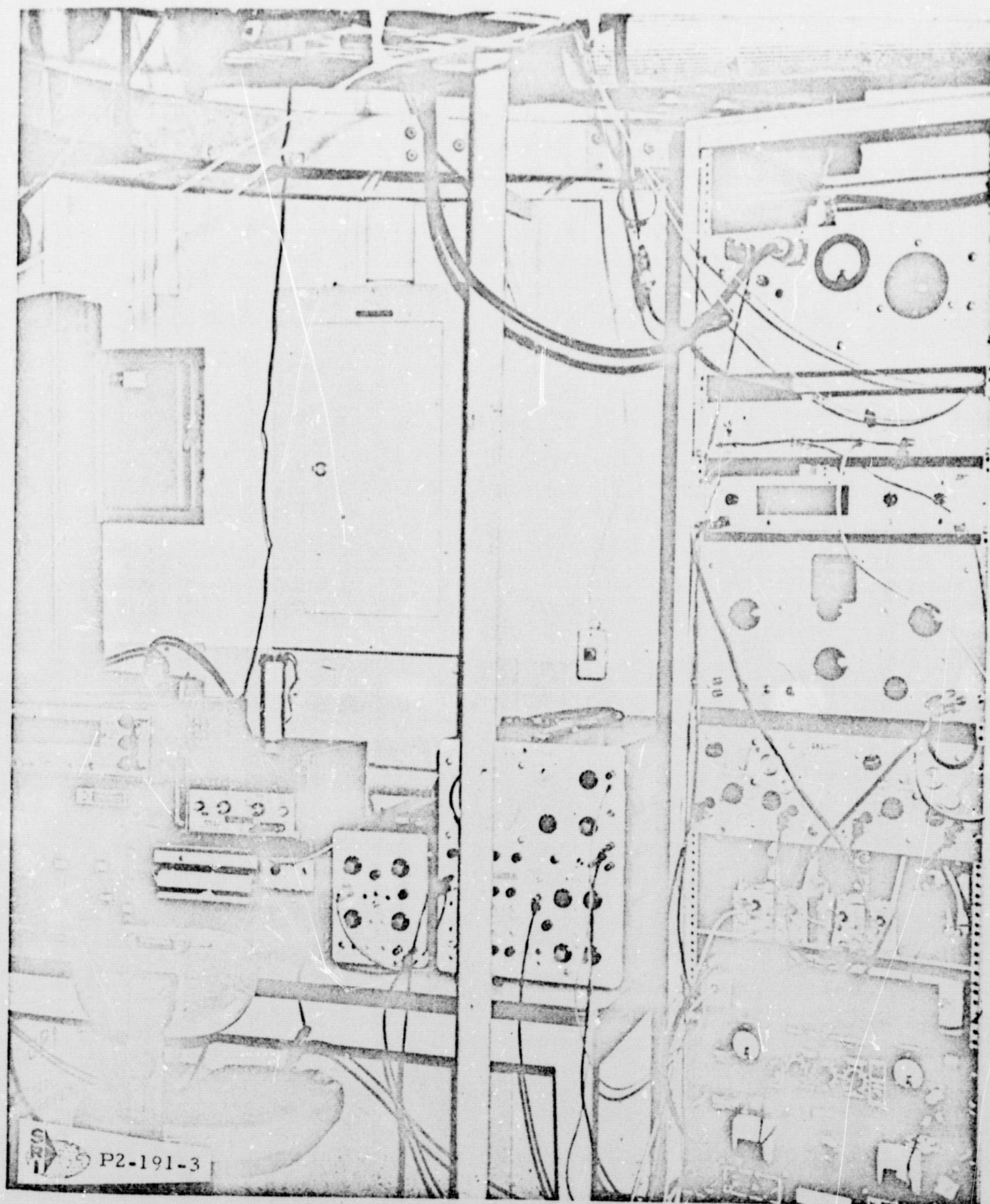


FIGURE 6. TEST INSTRUMENTATION

from the power source at the point of maximum slosh amplitude. The resulting slosh probe signal of the decaying slosh amplitude was recorded on a strip chart, and the entire process was then repeated several times for comparative purposes.

Next, the electromagnet was activated and the magnetic field intensity set at the desired level. (Incidentally, the magnet controls were at a remote location so that we had to transmit our instructions over an intercom.) We made a rough estimate of the effective gravity acting on the liquid by noting the change in the deadweight gage readout from the zero magnetic field reading and then correlating this change with the calibration curve to determine by how much the weight of the liquid had apparently decreased. After this, slosh and slosh decay tests were conducted as outlined above. We then reset the magnetic field to exactly zero and again read the change in the deadweight gage readout; in this way, the DC drift in the voltmeter reading during the test was evaluated.

A series of these kinds of tests were conducted, each time with an increased magnetic field, until the zero-g level seemed to have been exceeded.

One further point should be mentioned. All the calibration and slosh tests were run with full circulation of the magnet cooling water so that there would not be a variation in temperature of the test apparatus from test to test.* The circulating water created a lot of mechanical noise but this did not affect the tests materially since the electrical signals were filtered.

C. Data Reduction

Because the slosh resonant frequency, as a function of shake-table amplitude, was recorded directly, and the logarithmic slosh-damping coefficient could be obtained readily from the slosh-decay strip charts, the main data reduction effort was in correlating the effective gravity acting on the liquid as a function of applied magnetic field.

As mentioned earlier, the calibration curve for the deadweight gage gave an indication of the effective gravity, but we checked the accuracy of the curve in two ways. First, for a test run at a high gravity level (say about one-half or so of normal gravity, as indicated by the deadweight gage), we assumed that the recorded natural frequency was exactly equal to the theoretically predicted frequency (from one of the analyses given in Refs. 8, 9, 10 and 11) in order to obtain a theoretical gravity level (perhaps different from the experimental gravity level) that would produce exactly the observed natural frequency. Now, by using this "correct" gravity level and the observed

*River water at about 40°F was used for cooling (the tests were run during January 1970), while room temperature averaged about 65°F.

deadweight gage readout for the test in question and, in addition, the deadweight gage readout for normal gravity, we derived a corrected calibration curve to check the gravity levels at all other magnetic field levels. The difference between the two calibration curves was always very small. Secondly, since the magnetic liquid is completely magnetized or saturated at even low magnetic field levels, the effective gravities, g_{eff} , indicated by the calibration curve, were used to compute the liquid magnetization M_0 by the formula

$$M_0 = (g - g_{\text{eff}})/(\partial B_z/\partial z)$$

where $\partial B_z/\partial z$, the magnetic field gradient in the axial direction, is known from the magnet calibration curves for each magnetic field intensity B_0 . * If the calibration of g_{eff} were correct, the computed values of M_0 should not vary with B_0 , and, in fact, the computed values of M_0 were constant to within ± 1 percent, thereby verifying the g_{eff} computations.

Although we obtained consistent values of g_{eff} in this way; nonetheless, the combined effect of a minimum discrimination of about 0.3 gram in the measuring system and various inaccuracies, due to the electrical noise and DC drift, limited the accuracy of the predicted apparent liquid weight to about ± 0.5 gram. For the smaller tanks, 0.5 gram is about 3 to 5 percent of the total weight in normal gravity; consequently, the predicted gravity level had a "spread" of as much as 3 to 5 percent of normal gravity for these tanks.

*The origin of this equation is discussed in Section IV.

III. TEST RESULTS

As mentioned previously, our objectives were to determine the slosh natural frequency and viscous damping coefficients for tanks of various geometries, as a function of the effective gravity level.

A. Natural Frequency

Results for the three cylindrical tanks tested are plotted against gravity level and Bond number, $\rho g_{\text{eff}} R_0^2 / \sigma$, in Figures 7, 8, and 9, as well as theoretical curves (obtained from Refs. 8, 9) for comparison.* It can be seen that the test results for the 2.00- and 1.50-in.-diameter tanks compare very well to the theory, but for the 1.00-in. diameter tank, the uncertainties in g_{eff} , which are magnified for this small tank as explained earlier, made a quantitative comparison difficult even though the general trend is that test and theory are in agreement. Results for the one-half and three-quarters full spherical tank are plotted in Figures 10 and 11. Again, the comparison of theory (Refs. 10, 11) and experiment is very close. In none of the tests was there any significant dependence of natural frequency on excitation amplitude.

The lowest value of g_{eff} obtained in the tests was about 1 percent of standard gravity ($g_{\text{eff}}/g = 0.01$); the corresponding values of Bond number range from about 0.5 for the 1.00-in.-diameter tank, which is the smallest Bond number obtained in any of the tests, to about 2.0 for the largest cylindrical tank or the spherical tank. It was practically impossible to obtain smaller values of g_{eff} for several reasons. Since the electromagnet could not be adjusted much "finer" than about 500 gauss and since the apparent decrease in g_{eff} with increase in field strength was about 0.07 g per 1000 gauss at the fluid densities used (we used the smallest density fluid that could be made with the available parent magnetic fluid), the result was that g_{eff} could not be adjusted much more closely than 0.03 g except by a tedious trial-and-error process. Further, the least-count of our deadweight gage was about 0.3 gram, which, even for the tank containing the largest volume of liquid, corresponds to an uncertainty in g_{eff} of about ± 0.01 g.

B. Slosh Damping

The logarithmic decrements, δ , for the bare-wall slosh damping of the various tanks were computed from the amplitude-decay, strip-chart

*Measured properties of the magnetic fluid at 40°F are: kinematic viscosity, $\nu = 0.163 \text{ in}^2/\text{sec}$ ($1.05 \text{ cm}^2/\text{sec}$); surface tension $\sigma = 1.3 \times 10^{-4} \text{ lb/in.}$ (22.7 dynes/cm); and density ρ of about $2.60 \times 10^{-2} \text{ lb/in}^3$ (0.72 gram/cm^3), depending on the volume of the parent magnetic liquid diluted in the heptane solvent.

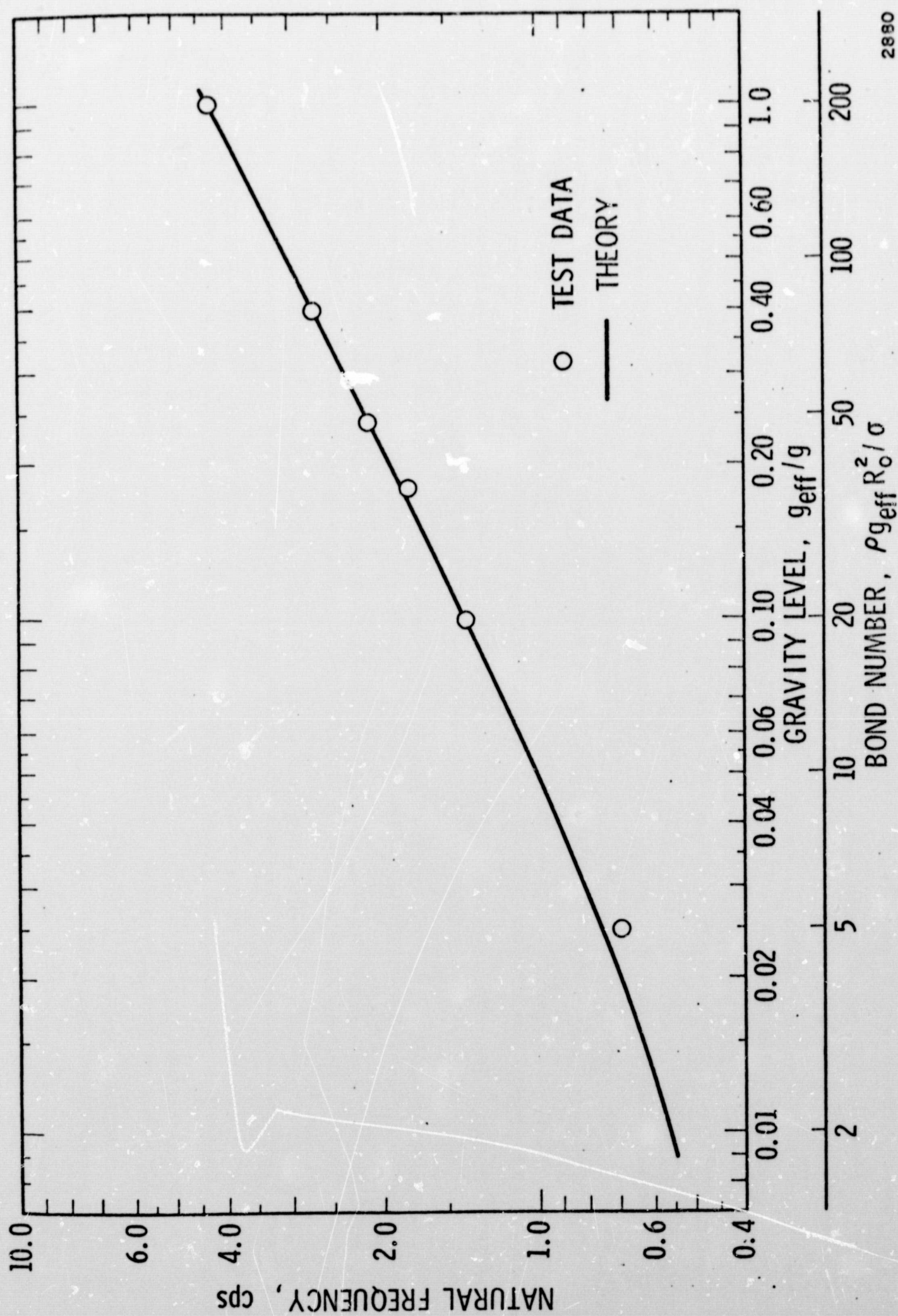


FIGURE 7. NATURAL FREQUENCY, 2.00-IN. CYLINDRICAL TANK

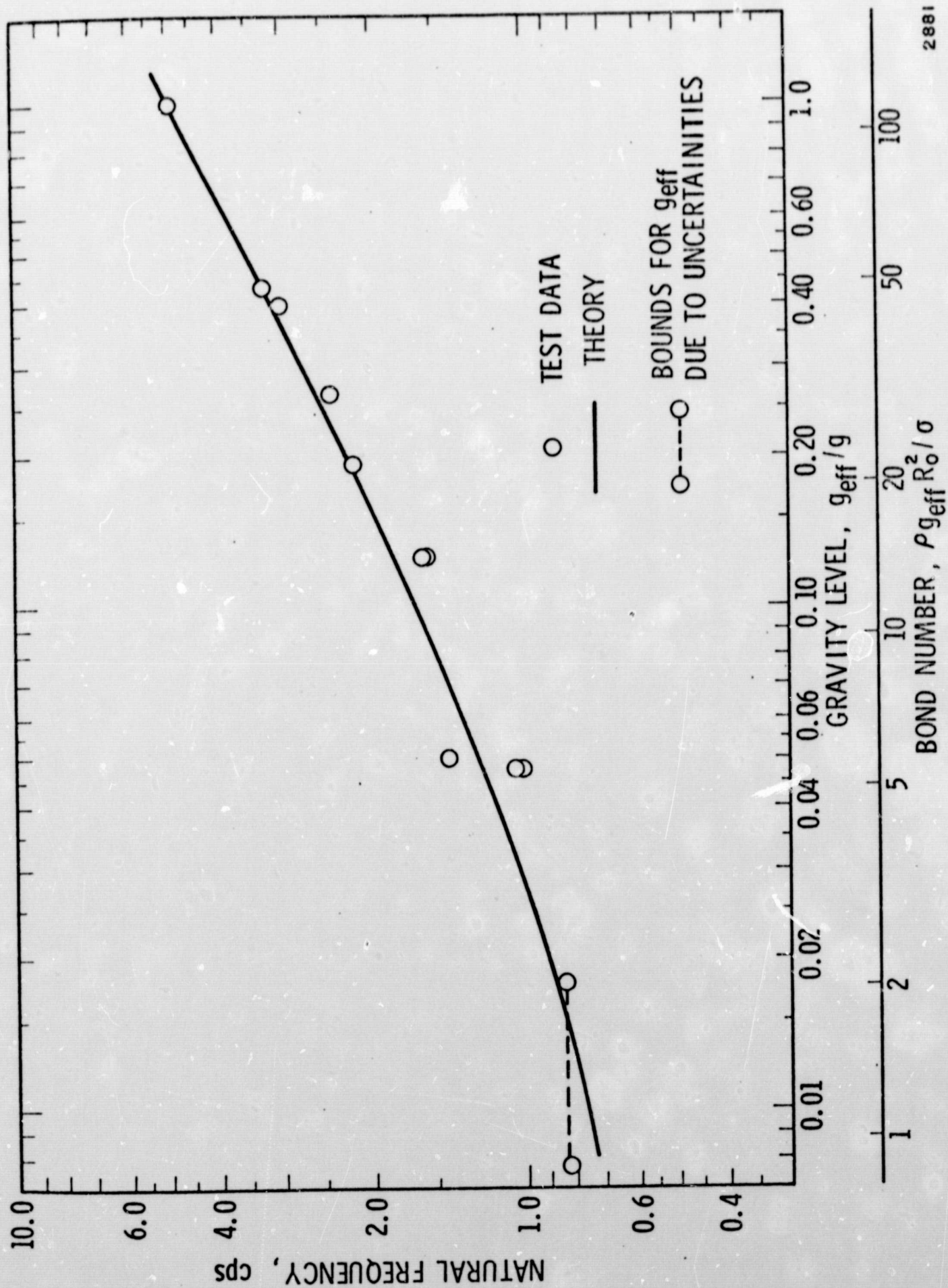


FIGURE 8. NATURAL FREQUENCY, 1.50-IN. CYLINDRICAL TANK

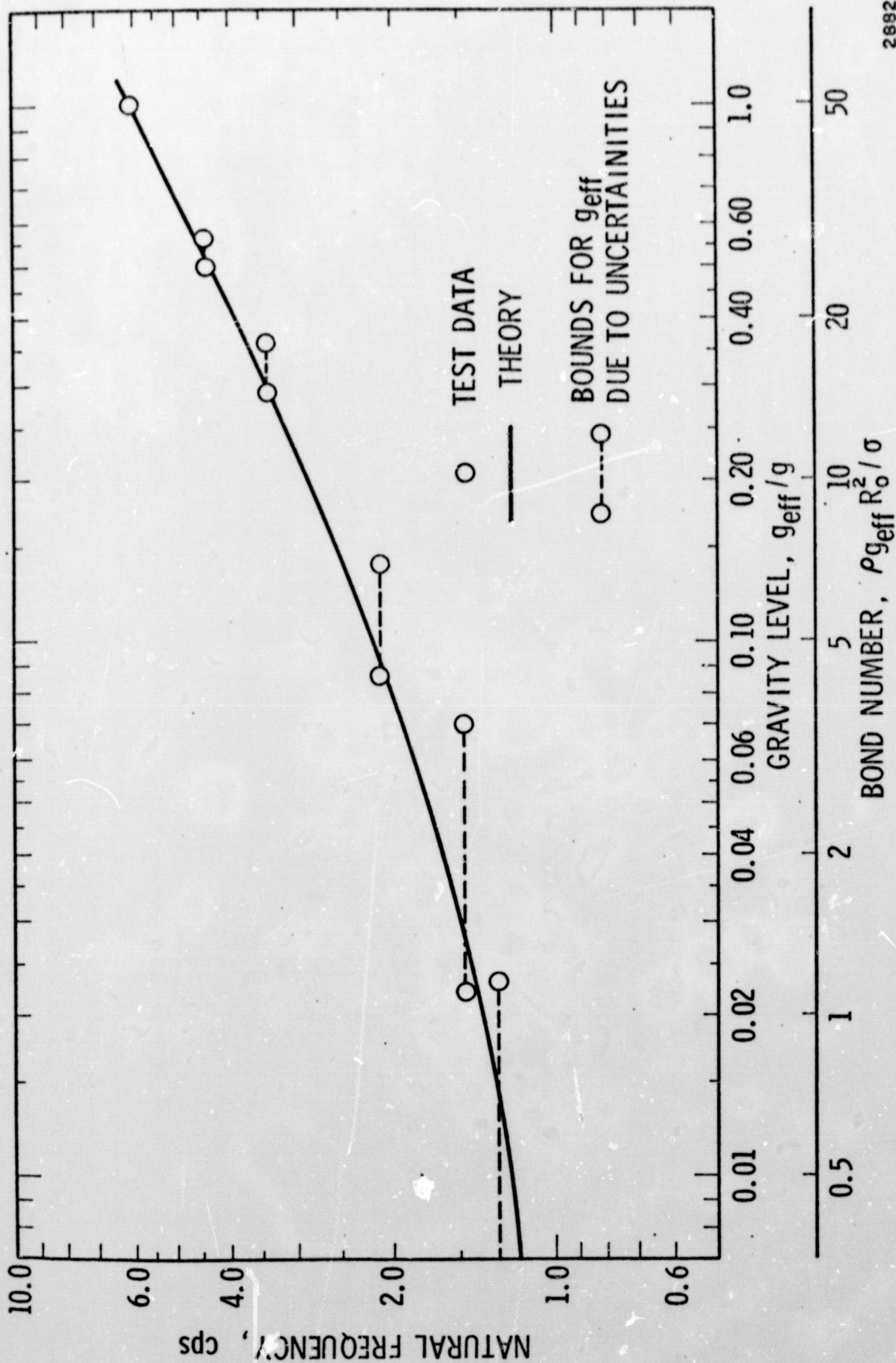


FIGURE 9. NATURAL FREQUENCY, 1.00-IN. CYLINDRICAL TANK

2892

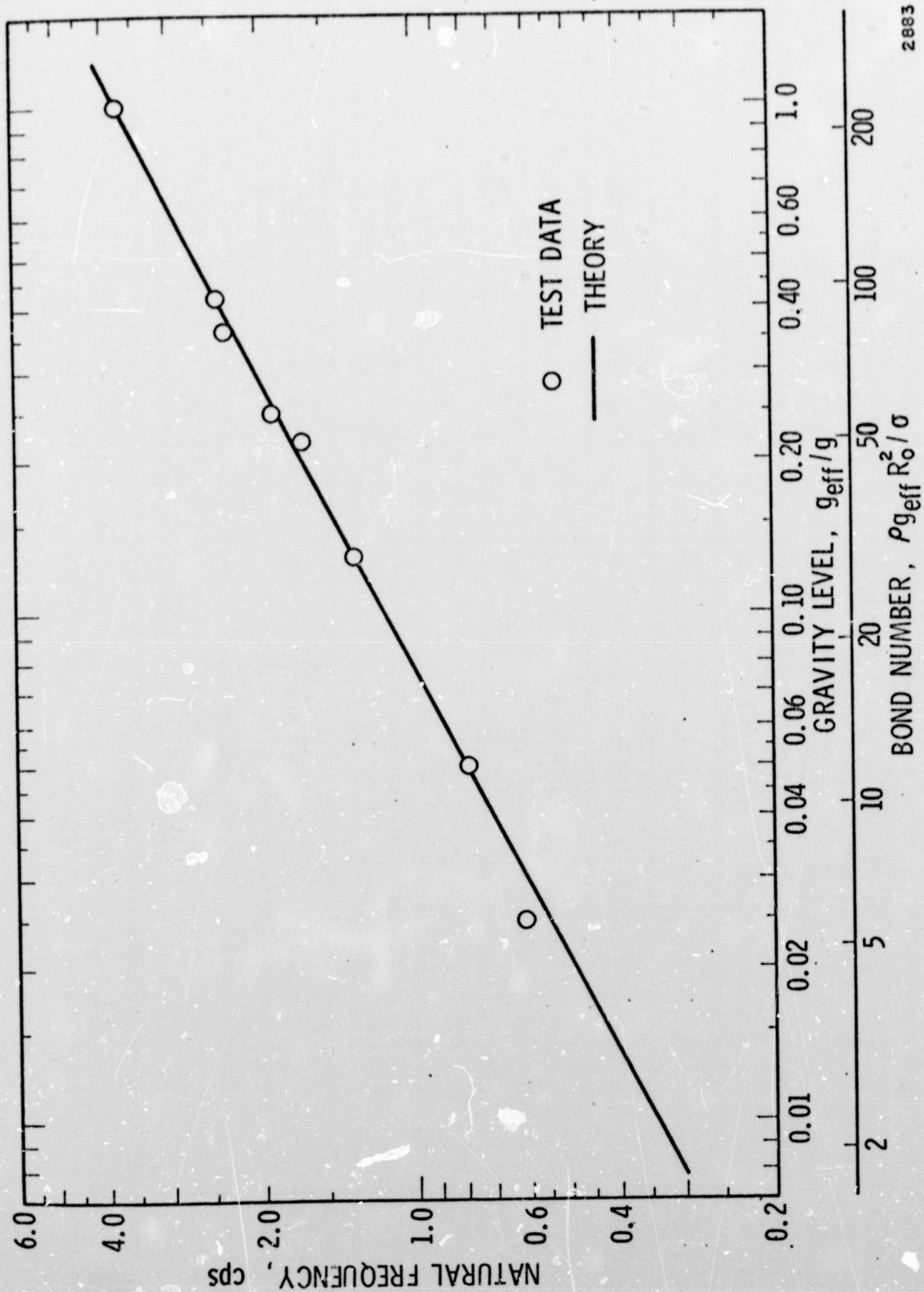
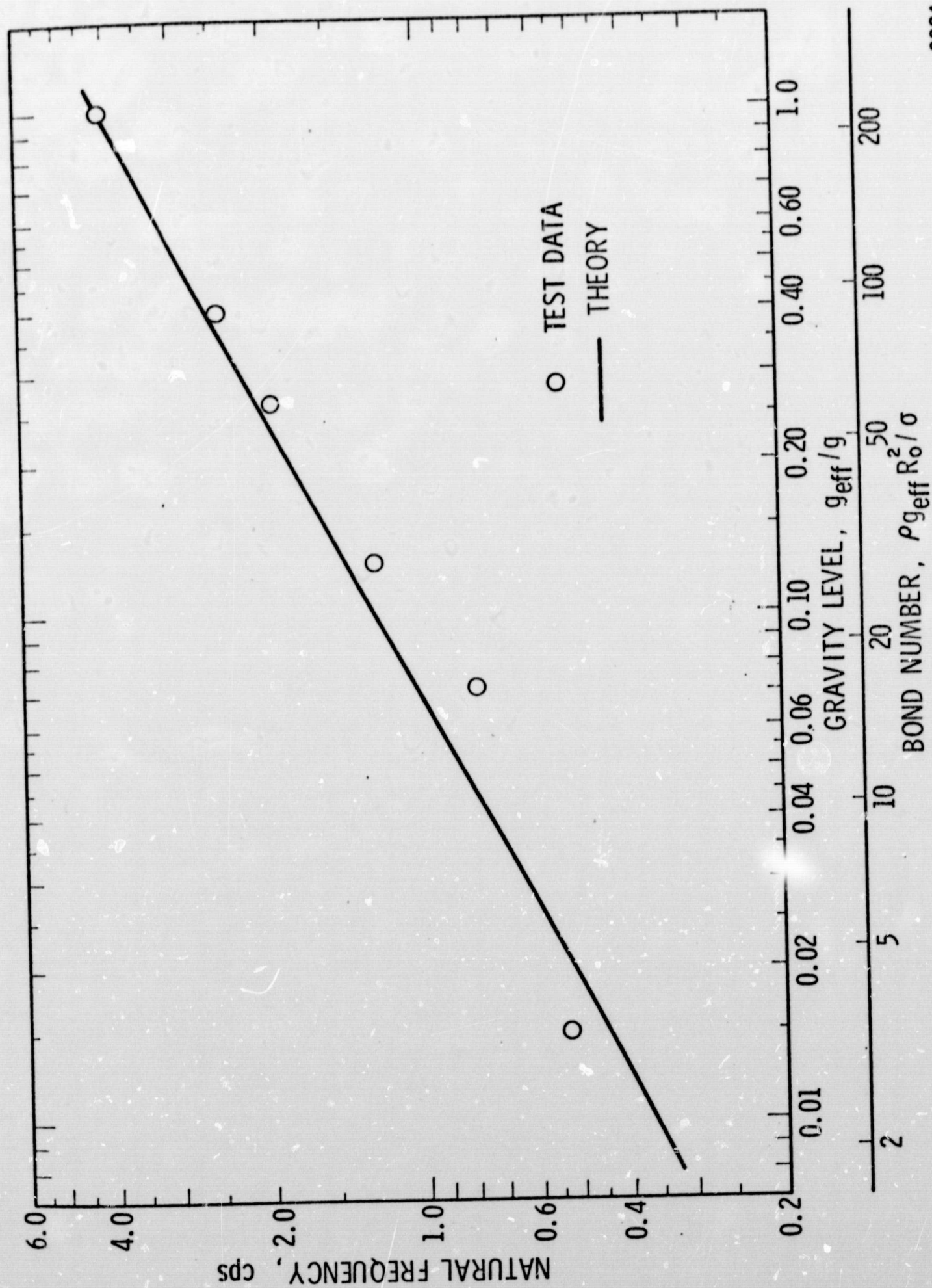


FIGURE 10. NATURAL FREQUENCY, 2.125-IN. SPHERICAL TANK, HALF-FULL



2884

FIGURE 11. NATURAL FREQUENCY, 2.125-IN. SPHERICAL TANK, THREE-QUARTERS FULL

records. Results for the 1.50-in.-diameter cylindrical tank and the three-quarters full spherical tank are shown plotted against gravity level and Galileo number, $R_o^{3/2} g_{eff}^{1/2} / \nu^{1/2}$, in Figures 12 and 13; the log decrements for the other tanks are similar.

As expected, the log decrements increased as the gravity level decreased. But the increase in δ was much greater than published correlations predict. For example, in Figure 11, the correlations

$$\delta = 4.98 (\nu^{1/2} R_o^{-3/4} g_{eff}^{-1/4})$$

(which is based on normal gravity tests, Ref. 12) and

$$\delta = 4.98 \nu^{1/2} R_o^{-3/4} g_{eff}^{-1/4} \left[1.0 + 8.2 (\rho g_{eff} R_o^2 / \sigma)^{-3/5} \right]$$

(which is based on low gravity simulations with small models, Ref. 13, and later verified by drop-tower tests, Ref. 14) both underestimate the damping encountered in our tests.

There are two possible reasons for these discrepancies. First, the apparent viscosity of a magnetic fluid increases in the presence of a magnetic field, by as much as 40 percent (as shown in Refs. 15 and 16), and the total increase in ν is attained, even for fields as low as 1000 gauss. This fact alone probably explains the rapid increase in δ above the expected value for $g_{eff}/g \geq 0.3$. Secondly, it is possible that eddy currents are induced in the iron particles of the fluid during the free-decay of the sloshing, which would increase the apparent viscous damping. We believe that no significant amount of energy is dissipated by this last process, since the particles are submicron in size; this belief is further supported by the fact that, in Figure 11, the slope of experimental data curve is about the same as the slope of the correlation equation (including Bond number effects) for $g_{eff} \leq 0.3$. In other words, after accounting for the increase in viscosity caused by the magnetic field in the range $1.0 \geq g_{eff}/g \geq 0.3$, the correlation equation does predict the observed δ variation with g_{eff} for $g_{eff}/g \leq 0.3$.

With regard to nonlinear effects, it appears that δ increases slightly as the excitation amplitude (i. e., slosh amplitude) increases, which is in agreement with other low-gravity simulations.

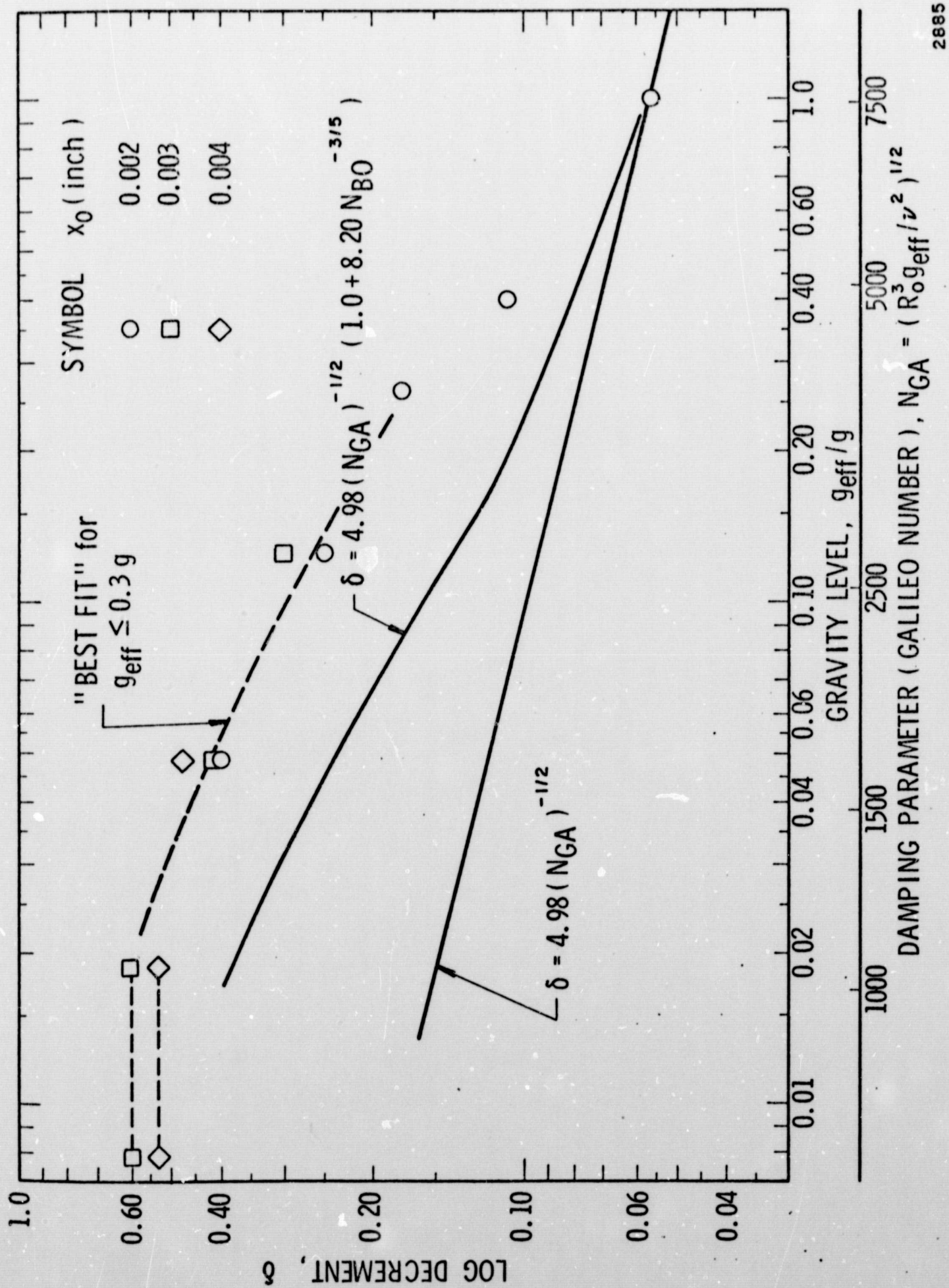
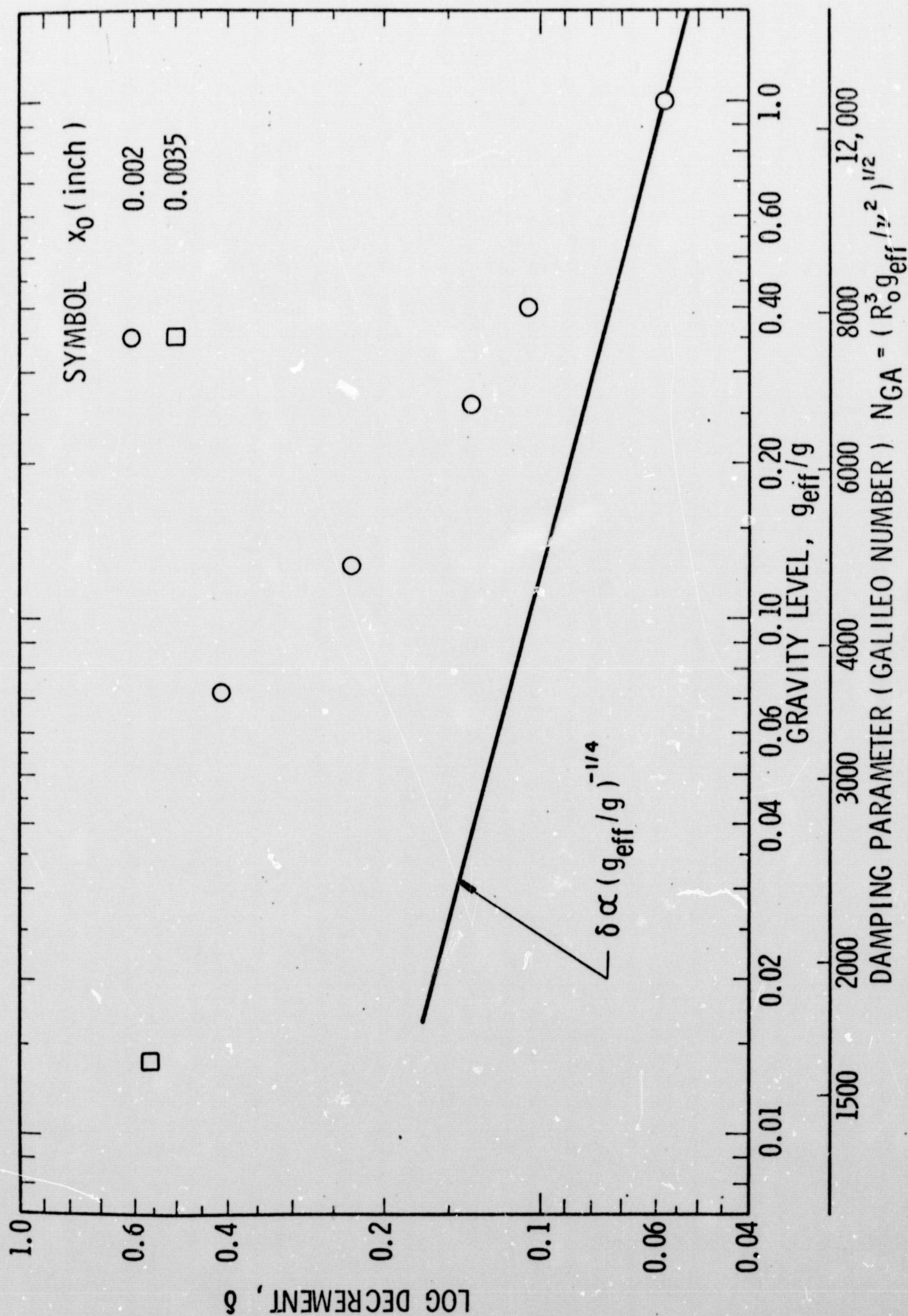


FIGURE 12. SLOSH DAMPING, 1.50-IN. CYLINDRICAL TANK



2886

FIGURE 13. SLOSH DAMPING, 2.125-IN. SPHERICAL TANK, THREE-QUARTERS FULL

IV. THEORY

In this section, a theory of magnetic fluid sloshing in solenoidal magnetic fields will be formulated by using the general theory of magnetic fluid dynamics developed in Refs. 3, 4, and 5, and particularly by Curtis, Ref. 7.

A. Basic Equations

Only two basic equations of ideal-flow theory are affected by the magnetic interaction terms: the equation of motion, and the boundary condition relating to pressure balance at a free surface.

The equation of motion for a magnetic liquid is

$$\frac{\partial \vec{V}}{\partial t} + \vec{V} \cdot \nabla \vec{V} = -\frac{1}{\rho} \nabla p - g \vec{a}_z + \vec{M} \cdot \nabla \vec{B} \quad (1)$$

where \vec{M} (amperes/meter) is the induced magnetization of the fluid, \vec{B} (webers/meter²)* is the applied magnetic field, and the other quantities must be measured in a meter-kilogram-second system of units. The coordinate axes, as shown in Figure 14, have the positive z-axis upwards, and \vec{a}_z is the unit vector in the z direction.

The change in the pressure balance at a free surface is due to the discontinuity in \vec{M} at the free surface, which induces a jump in pressure of magnitude $1/2 \mu_0 (\vec{M} \cdot \vec{n})^2$ across the surface, ($\mu_0 = 4\pi \times 10^{-7}$ webers/ampere-meter is the "permeability of free space" and \vec{n} is the unit vector normal to the free surface).

B. Magnetic Body-Force Potential

Since it can be shown that $\vec{M} \times \vec{B} = 0$, the magnetically induced body-force $\vec{M} \cdot \nabla \vec{B}$ in the equation of motion, can be derived from a potential, say $\vec{M} \cdot \nabla \vec{B} = \nabla \psi$; of course, the gravitational body force is also derivable from a potential, which, in this case, is just $-gz$.

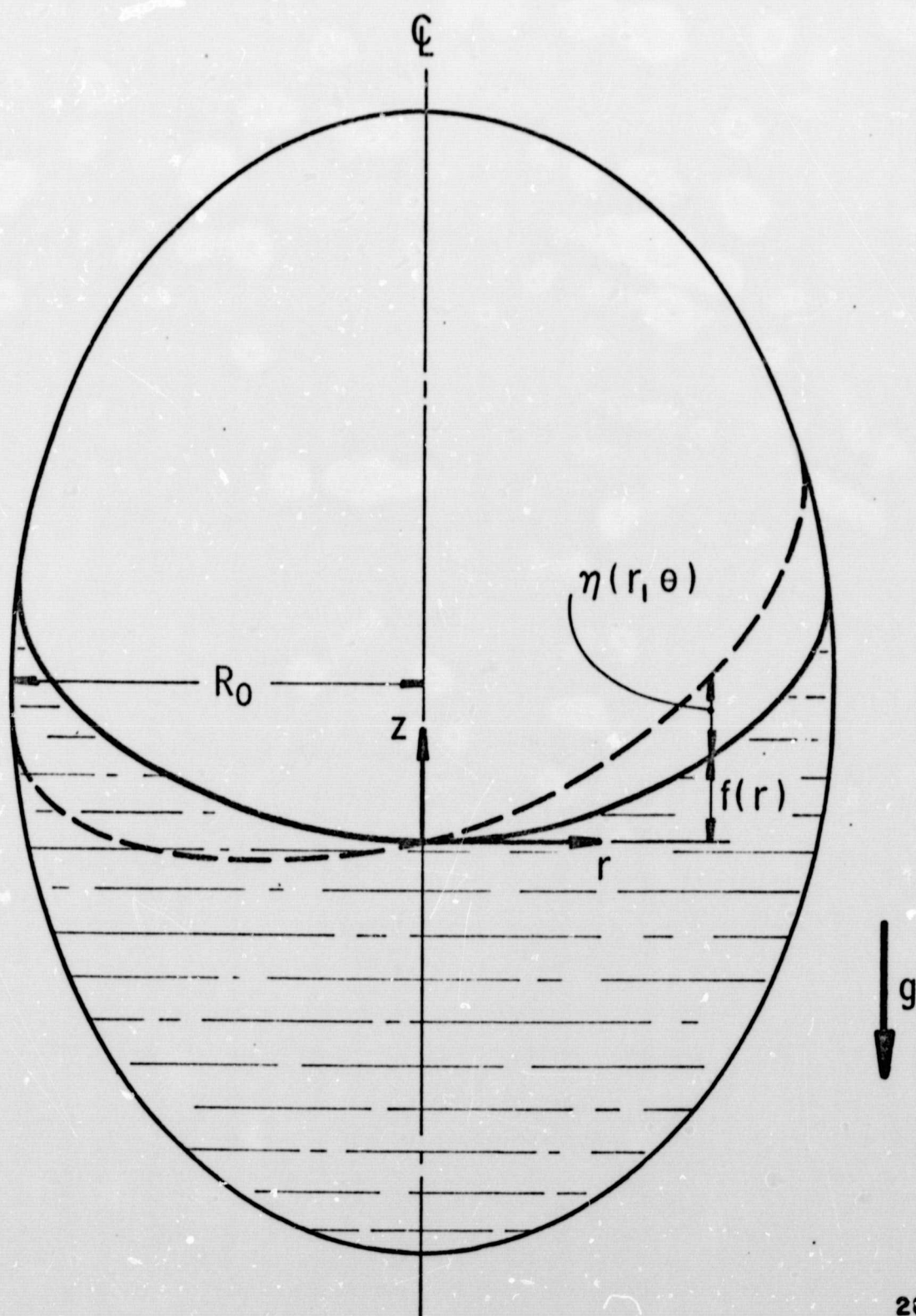
For the NASA-110-kilogauss electromagnet, the magnetic field at the test location has a radial and an axial component (Ref. 17):

$$B_z = 0.55 B_0 + 4.45 R_0 B_0 (z/R_0) \quad (2)$$

$$B_r = -2.22 R_0 B_0 (r/R_0) \quad (3)$$

which are both correct to a very close approximation. Also, B_0 , the axial field at the center of the magnet, is the magnetic field measured in our tests.

*1 weber/meter² = 10,000 gauss.



2077

FIGURE 14. NOMENCLATURE FOR ANALYSIS

Because \vec{M} is parallel to \vec{B} , the magnetization vector is

$$\vec{M} = M_0(B_r \vec{a}_r + B_z \vec{a}_z) / (B_r^2 + B_z^2)^{1/2} \quad (4)$$

where M_0 is the magnitude of the vector \vec{M} . Thus, since $\partial B_r / \partial z = \partial B_z / \partial r = 0$ [see Eqs. (2) and (3)], $\vec{M} \cdot \nabla \vec{B}$ can be written in component form as

$$\vec{M} \cdot \nabla \vec{B} = M_0 \left[B_z \frac{dB_z}{dz} \vec{a}_z + B_r \frac{dB_r}{dr} \vec{a}_r \right] / (B_r^2 + B_z^2)^{1/2} \quad (5)$$

We will show below that M_0 is independent of \vec{B} , which is the same as saying that the liquid is fully magnetized, or "saturated," for all the \vec{B} fields of interest here. Realizing this, it can be checked by direct differentiation that the magnetic body-force potential is

$$\psi(r, z) = M_0(B_r^2 + B_z^2)^{1/2} - 0.55 M_0 B_0 \quad (6)$$

The constant term, $0.55 M_0 B_0$, has been added for convenience in the following analysis; of course, any constant can be added to or subtracted from ψ without affecting $\nabla \psi$, which is the quantity of interest.

Now, by substituting Eqs. (2) and (3) into the definition of ψ , it can be seen that the effective gravitational acceleration in the z -direction is

$$g_{\text{eff}} = \frac{\partial}{\partial z} (gz - \psi) = g - 0.11 \left(\frac{M_0 B_0}{R_0} \right) \left\{ \frac{1 + 0.2z/R_0}{[(1 + 0.2z/R_0)^2 + 0.01(r/R_0)^2]^{1/2}} \right\}$$

Since $(r/R_0)^2 \leq 1$ and $(1 + 0.2z/R_0)^2$ is of the order of magnitude of 1, we can approximate Eq. (7) very closely by

$$g_{\text{eff}} \approx g - 0.11 M_0 B_0 / R_0 \quad (8)$$

for the purpose of calculating M_0 . Using the experimentally measured set of values of g_{eff} and B_0 , we have used Eq. (8) to verify that M_0 is in fact independent of B_0 for any B_0 greater than about 1000 gauss (and all of our data tests were run at fields greater than 4000 gauss). In addition, we have used the "equation-of-state" $\vec{M} = f(\vec{B})$ proposed by Curtis, Ref. 7, along with some order-of-magnitude estimates of the magnetic moment of each sub-micron iron particle to show analytically that the magnetic fluid saturates at about 1000 gauss. These two independent checks demonstrate that it is legitimate to assume M_0 to be independent of B_0 .

A typical value of M_0 obtained from Eq. (8) is 1000 amperes/meter, but M_0 varied slightly from one set of tests to another because of slight variations in the volume of magnetic liquid dissolved in the heptane from one test setup to another.

C. Equilibrium Free Surface

In the absence of sloshing, the pressure p at a point on the free surface in the liquid differs from the air pressure p_a outside the free surface because of both the surface tension and the magnetic interaction at the surface mentioned previously. Thus, a pressure balance at the free surface yields

$$p + \sigma \left(\frac{1}{R_1} + \frac{1}{R_2} \right) + \frac{1}{2} \mu_0 M_n^2 - \rho g z + \rho \psi = p_a \quad (9)$$

where $M_n = \vec{M} \cdot \vec{n}$ and R_1 and R_2 are the principal radii of the surface curvature.

The magnetic body-force potential, ψ , induces a radial variation in the static pressure which thereby causes the surfaces of constant pressure to be curved, and not level and perpendicular to the z -axis as they should be in a uniform gravitational field. The new "level" lines of constant pressure are given by

$$-gz + \psi = K = \text{constant} \quad (10)$$

[The reader is cautioned not to identify the constant on the right-hand side of Eq. (10) directly with the pressure since any constant can be added freely to the definitions of the potentials on the left-hand side. In particular, $K = 0$ does not necessarily correspond to $p = 0$ at the free surface.]

Since $g_{\text{mag}} = 0.11 M_0 B_0 / R_0$ is the effective decrease in gravity [that is, $g_{\text{eff}} = g - g_{\text{mag}}$ from Eq. (8)], Eq. (10) can be written as

$$K = -gz + 5R_0 g_{\text{mag}} [(1 + 0.2z/R_0)^2 + 0.01(r/R_0)^2]^{1/2} - 5R_0 g_{\text{mag}} \quad (11)$$

The maximum deflection of the constant pressure lines from the horizontal occurs for $g_{\text{mag}} = g$. The equation of the free surface can be derived from the general solution of Eq. (11), for this case of $g_{\text{eff}} = 0$, by evaluating the constant K so that the volume of the contained fluid is equal to $\pi R_0^2 h$ where h is the average liquid depth. This equation works out to be

$$(z/R_0)_{\text{free surface}} = \frac{h}{R_0} - \left[\frac{0.012}{1 + 0.2(h/R_0)} \right] (r/R_0)^2 \quad (12)$$

Thus, the maximum deflection of the free surface, due to the static radial pressure gradient, is only about 1 percent, even when the effective gravity level is zero. *

We will now measure the vertical coordinate of a point in the liquid from the slightly curved, imaginary free surface that is determined by the above considerations. In this coordinate system, the radial variation of pressure falls out of Eq. (9), so that now Eq. (9) is

$$p + \sigma \left(\frac{1}{R} + \frac{1}{R_2} \right) + \frac{1}{2} \mu_0 M_n^2 - \rho(g - g_{\text{mag}}) z = p_a \quad (9')$$

Evaluating this equation at $r = 0$, $z = 0$, and subtracting the result from Eq. (9') gives

$$\sigma \left(\frac{1}{R_1} + \frac{1}{R_2} \right) - \sigma \left(\frac{1}{R_1} + \frac{1}{R_2} \right) \Big|_{r=0} + \frac{1}{2} \mu_0 (M_n^2 - M_n^2 \Big|_{r=0}) - \rho g_{\text{eff}} f = 0 \quad (13)$$

where $z = f(r)$ is the equation of the free surface. In nondimensional terms, the axisymmetric form of this equation is

$$\frac{1}{R} \frac{d}{dR} \left\{ \frac{R dF/dR}{[1 + (dF/dR)^2]^{1/2}} \right\} - 2 \frac{d^2 F}{dR^2} \Big|_{R=0} - N_{\text{BO}} F - N_{\text{MI}} \left[\frac{(dF/dR)^2}{1 + (dF/dR)^2} \right] = 0 \quad (14)$$

where $F = f/R_0$, $R = r/R_0$, $N_{\text{BO}} = \rho g_{\text{eff}} R_0^2 / \sigma$, and $N_{\text{MI}} = \mu_0 M_0^2 R_0 / 2$. [We have neglected the slight variation of \bar{M} with R in deriving Eq. (14) although this is not a necessity.]

For the 1.5-in. (3.81-cm) diameter cylindrical tank, a typical value of $N_{\text{MI}} = 0.5$. Consequently, when g_{eff} is small, so that $N_{\text{BO}} \leq 1$, N_{MI} and N_{BO} will be comparable in magnitude, and it appears that the free surface of the magnetic fluid will be somewhat different from the normal low- g free surface. The magnitude of the difference cannot be easily estimated from

*It should be mentioned that $g_{\text{eff}} = -g + \partial\psi/\partial z$ is not exactly zero throughout the fluid for this case, as can be seen from Eq. (7). This slight variation of pressure with depth, in fact, is what allows the even smaller variation of pressure with radial position to be balanced; otherwise, the liquid would all collect along the axis, $r = 0$.

Eq. (14) short of a complete numerical solution, and we did not measure the free-surface shape in our experiments; nonetheless, the good agreement of our tests to normal low-g sloshing theory, even for $N_{BO} \approx 1$, seems to indicate that the effect of the difference in the free-surface shape is not large in the final results.

D. Sloshing Analysis

By integrating the equation of motion, Eq. (1), to get Bernoulli's equation for a magnetic liquid, and by evaluating this equation at the equilibrium free surface, the pressure-velocity boundary condition at the free surface can be shown to be

$$\begin{aligned} (\rho/\sigma) \frac{\partial \phi}{\partial t} + (\rho/\sigma) \left[g - \frac{\partial \psi}{\partial z} \right] \eta - \frac{1}{r} \frac{\partial}{\partial r} \left\{ \frac{r \partial \eta / \partial r}{[1 + (df/dr)^2]^{3/2}} \right\} \\ - \frac{1}{r^2} \frac{\partial}{\partial \theta} \left\{ \frac{\partial \eta / \partial \theta}{[1 + (df/dr)^2]^{1/2}} \right\} - \frac{\rho \mu_0 M_0^2}{\sigma} \left\{ \frac{df/dr}{[1 + (df/dr)^2]^2} \right\} \frac{\partial \eta}{\partial r} = 0 \quad (15) \end{aligned}$$

where η is the wave height measured above the equilibrium free surface. Equation (15) has been linearized with respect to ϕ and ψ . This is the only equation for a magnetic fluid that differs from the usual nonmagnetic fluid equations.

Since $\partial \psi / \partial z$ is constant to a very good approximation and equal to g_{mag} , Eq. (12) in nondimensional form is

$$\begin{aligned} -\Omega^2 \Phi + N_{BO} H - \frac{1}{R} \frac{\partial}{\partial R} \left\{ \frac{R \partial H / \partial R}{[1 + (dF/dR)^2]^{3/2}} \right\} \\ - \frac{1}{R^2} \frac{\partial}{\partial \theta} \left\{ \frac{\partial H / \partial \theta}{[1 + (dF/dR)^2]^{1/2}} \right\} - 2N_{MI} \left\{ \frac{dF/dR}{[1 + (dF/dR)^2]^2} \right\} \frac{\partial H}{\partial R} = 0 \quad (16) \end{aligned}$$

which, as before, is the same as the standard low-g theory except for the last term. The magnitude of this term is believed to be small because dF/dR is small near $R = 0$ and very large near $R = 1$ (in fact, $dF/dR = \infty$ at $R = 1$ for a zero-degree constant angle) so that over nearly the entire free surface the factor multiplying N_{MI} is nearly zero. In any event, the effect of this magnetic interaction at the surface was not noticeable in our test results.

V. CONCLUSIONS AND RECOMMENDATIONS

We have demonstrated in this exploratory study of liquid sloshing that low-gravity fluid mechanics can be accurately examined experimentally by the magnetic-fluid method. The slosh natural frequency results, for example, show very little deviation from true low-gravity theoretical predictions even for a simulated gravity as low as 0.01 g; this is a much smaller gravity level and Bond number than can be obtained by any method other than drop-tower tests, which are extremely time-limited.

The natural frequency and other characteristics of low-gravity sloshing were duplicated well in our tests, but the measured slosh damping was significantly greater than previous, low-gravity simulations have shown it to be. We believe this discrepancy is caused by the increase in the apparent viscosity of a magnetic liquid in a magnetic field. Consequently, accurate slosh damping data cannot be obtained from the magnetic fluid simulation.

We have also presented a theory of magnetic fluid sloshing in solenoidal magnetic fields. This theory tends to indicate that for a very low effective gravity (where the Bond number is less than one) magnetic fluid sloshing will deviate from true low-gravity behavior. The discrepancy is due primarily to a magnetic force at the free surface, similar to surface tension, which induces a jump in fluid pressure across the free surface. We believe the effect of this force to be small, but its actual magnitude cannot be estimated analytically without a complete numerical solution of the equations of motion.

The experimental program can be extended to lower effective gravities, and certainly less than 0.01 g, by improving our experimental apparatus in order to give a more accurate indication of the apparent weight of the contained liquid. Further improvements could be obtained by using an electromagnet with a smaller maximum field. Zero gravity can be obtained with much smaller fields than the maximum field of 110 kilogauss of the electromagnet used in our tests. (We never required more than 15 kilogauss.) A smaller electromagnet would presumably have more precise controls and thereby allow the effective gravity level to be changed by smaller increments than was possible in our tests.

It would be valuable to investigate the theoretical limitations of the magnetic fluid simulation. This investigation would involve obtaining numerical solutions to the theory presented in this report and then comparing the results to theories for true low-gravity sloshing.

LIST OF REFERENCES

1. Papell, Stephen S. and Faber, Otto C., Jr., "Zero- and Reduced-Gravity Simulation on a Magnetic-Colloid Pool-Boiling System," NASA TN D-3288, February 1966.
2. Dodge, Franklin T., "A Discussion of Laboratory Methods of Simulating Low-Gravity Fluid Mechanics," Tech. Rept. No. 3, Contract NAS8-20290, Southwest Research Institute, San Antonio, Texas, February 1967.
3. Neuringer, Joseph L. and Rosensweig, Ronald E., "Ferrohydrodynamics," Physics of Fluids, 7, December 1964, pp 1927-37.
4. Rosensweig, Ronald E., "Buoyancy and Stable Levitation of a Magnetic Body Immersed in a Magnetizable Fluid," Nature, 210, May 7, 1966, pp 613-14.
5. Rosensweig, Ronald E., "Magnetic Fluids," International Science and Technology, July 1966, pp 48-56.
6. Papell, Stephen S. and Faber, Otto C., Jr., "On the Influence of Nonuniform Magnetic Fields on Ferromagnetic Colloidal Sols," NASA TN D-4676, August 1968.
7. Curtis, Richard A., "Magnetic Fluid Dynamics," Ph. D. Dissertation, Department of Aeronautical Engineering, Cornell University, Ithaca, New York, 1968.
8. Dodge, Franklin T. and Garza, Luis R., "Experimental and Theoretical Studies of Liquid Sloshing at Simulated Low Gravities," Trans. ASME, J. Applied Mechanics, 34, June 1968, pp 267-73.
9. Concus, P., Crane, G. E., and Satterlee, H. M., "Small Amplitude Lateral Sloshing in a Cylindrical Tank with a Hemispherical Bottom Under Low Gravitational Conditions," NASA CR-54700, January 1967.
10. Concus, P., Crane, G. E., and Satterlee, H. M., "Small Amplitude Lateral Sloshing in Spheroidal Containers Under Low Gravitational Conditions," NASA CR-72500, February 1969.
11. Chu, Wen-Hwa, "Low Gravity Fuel Sloshing in an Arbitrary Axisymmetric Rigid Tank," ASME Paper 70-APM-EEE (to appear, Trans. ASME, J. Applied Mechanics).

12. The Dynamic Behavior of Liquids in Moving Containers, H. N. Abramson (ed), NASA SP-106, 1966.
13. Dodge, Franklin T. and Garza, Luis R., "Simulated Low-Gravity Sloshing in Cylindrical Tanks Including Effects of Damping and Small Liquid Depth," NASA CR-61469, December 1967.
14. Salzman, Jack A. and Masica, William J., "Lateral Sloshing in Cylinders Under Low-Gravity Conditions," NASA TN D-5058, February 1969.
15. McTague, John P., "Magnetoviscosity of Magnetic Colloids," J. Chemical Physics, 51, July 1969, pp 133-36.
16. Hall, W. F. and Busenberg, S. N., "Viscosity of Magnetic Suspensions," 51, July 1969, pp 137-44.
17. Brown, Gerald Y., Flax, Lawrence, Itean, Eugene C., and Lawrence, James C., "Axial and Radial Magnetic Fields of Thick, Finite-Length Solenoids," NASA TR R-170, 1963.